ACS APPLIED MATERIALS & INTERFACES

Research Article

www.acsami.org

Focal Contact Formation of Vascular Smooth Muscle Cells on Langmuir–Blodgett and Solvent-Cast Films of Biodegradable Poly(ester amide)s

Darryl K. Knight,[†] Rebecca Stutchbury,[‡,§] Daniel Imruck,[§,⊥] Christopher Halfpap,[§,⊥] Shigang Lin,[†] Uwe Langbein,[⊥] Elizabeth R. Gillies,[†,‡] Silvia Mittler,[§] and Kibret Mequanint*[,†]

[†]Department of Chemical and Biochemical Engineering, [‡]Department of Chemistry, [§]Department of Physics and Astronomy, The University of Western Ontario, London, Ontario, Canada

[⊥]Department of Physics and Institute for Microtechnologies, The University of Applied Sciences RheinMain, Am Brückweg 26, 65428 Rüsselsheim, Germany

Supporting Information

ABSTRACT: The ability of biomaterials to support the adhesion of cells is a necessary condition for their use in scaffold-guided tissue engineering. Waveguide evanescent field fluorescence (WEFF) microscopy is a relatively new microscopic technique that allows the number of cell adhesions to a waveguide surface be measured by imaging the interfacial contact region between the cells and their substratum. In this work, the adhesion of human coronary artery smooth muscle cells (HCASMCs) to ultrathin films (20 nm) of poly(ester amide)s (PEAs) prepared by Langmuir–Blodgett (LB) technology on waveguides was investigated and compared with conventional vinculin immunostaining on solvent cast PEA films. Cell culture was conducted both in the presence and absence of serum to evaluate the effect of nonspecific protein adsorption that mediates cell adhesion. WEFF microscopy analyses revealed that the cationic PEA enhanced the number of attachment sites compared with the control waveguides regardless of the culture medium. Although differences in cell adhesions between different PEAs were suggested by the results, no statistically significant differences were found. Similar results were observed with presently and previously reported vinculin immunostaining studies, further validating the use of WEFF microscopy to quantify cell adhesions. Moreover, the focal adhesions of the HCASMCs to the PEA surfaces indicate these PEAs can promote integrin signaling, which is vital in cell survival, migration, and proliferation, and ultimately in scaffold-guided vascular tissue engineering.

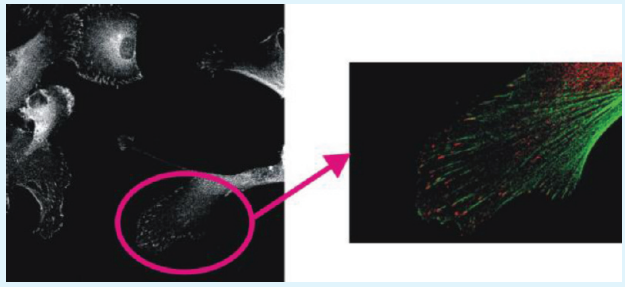

KEYWORDS: *waveguide evanescent field fluorescence (WEFF) microscopy, Langmuir–Blodgett (LB) films, poly(ester amide)s (PEAs), human coronary artery smooth muscle cells (HCASMCs), vinculin immunostaining, focal adhesions*

INTRODUCTION

With the aim of successfully engineering scaffold-guided tissues, there is an ever-increasing interest in the interactions of cells with both synthetic and natural biomaterials.[1,2] When cells are seeded onto a biomaterial, both nonspecific and receptor-mediated cell interactions between various molecules on the cell membrane and chemical groups on the biomaterial determine the fate of cell adhesion, spreading, proliferation, and differentiation.[3] In view of this, the study of the contact regions between a cell and its substratum is of considerable interest as its investigation provides useful information about the cytocompatibility of the substratum and the affinity of cells toward that particular surface. Although information concerning these interactions is often inferred from enzyme-linked immunosorbent assays (ELISA) and immunostaining of focal adhesion molecules,[4] different microscopic techniques such as total internal reflection fluorescence (TIRF),[5,6] surface plasmon resonance microscopy (SPRM),[7] interference reflection microscopy (IRM),[8] and fluorescence interference-contrast (FLIC) microscopy[9] have also been used.

Recently, waveguide evanescent field fluorescence (WEFF) microscopy was developed with the capability to image cell-substratum contact regions with certain advantages.[10−15] In WEFF microscopy, waveguides are implemented as microscopy substrates. The generation of an evanescent field of up to ∼70 nm in depth from the waveguide surface enables the excitation of fluorescent dyes located in the cells within this range only. Because of evanescent field decay beyond ∼70 nm, the remainder of the cell is not illuminated and thus does not contribute to the image. It has been established that WEFF and TIRF microscopy can deliver comparable information.[13] However, the key advantages of WEFF microscopy are that

Received: November 13, 2011
Accepted: February 13, 2012
Published: February 13, 2012

Scheme 1. Structures of PEAs 1−3[a]

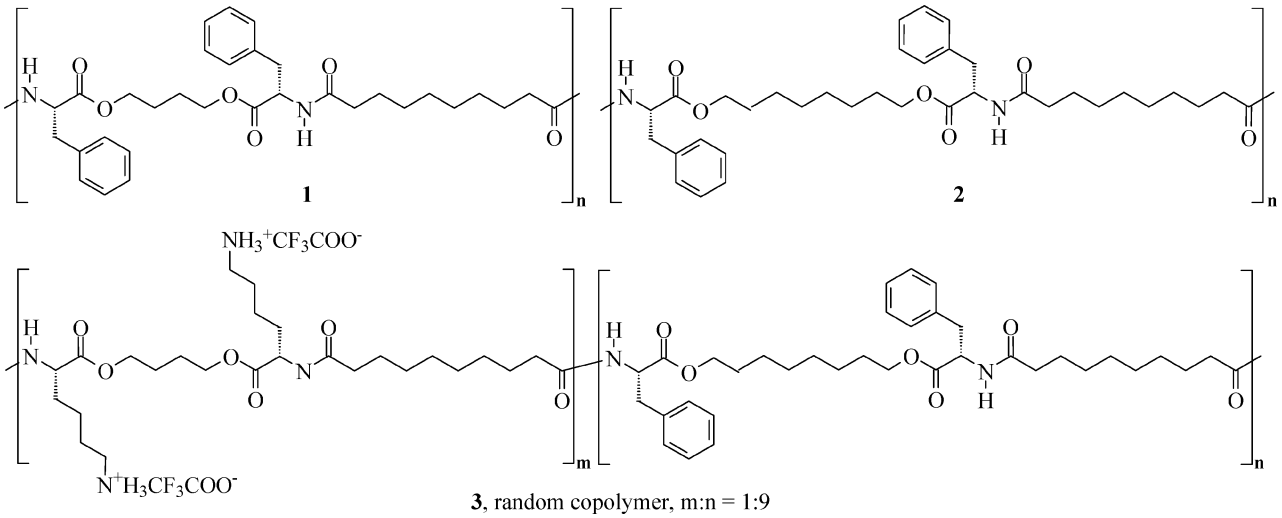

[a]PEA **3** is a random copolymer where 10 mol % of L-phenylalanine was randomly replaced by L-lysine.

biomaterials can be easily coated on to the surface of the waveguide and that the user can freely choose the field of view and the magnification during an experiment.[12,14] As WEFF microscopy restricts the distance above the waveguide to ∼70 nm, it necessitates the fabrication of ultrathin films of the material being tested for cell adhesion.

The objectives of the present work were 2-fold: (i) to prepare Langmuir−Blodgett (LB) films from three different poly(ester amide)s (PEAs) on waveguide substrates and, (ii) to describe the use of WEFF microscopy for investigating human coronary artery smooth muscle cell (HCASMC) adhesions on LB PEA films to compare it with a conventional immunostaining approach. The class of biodegradable PEAs used in this study is of significant interest for the development of a wide range of biomedical applications as the incorporation of naturally occurring α-amino acids enables the syntheses of functional biomimetic materials. Recently, our group has been investigating the potential of PEAs to serve as vascular tissue engineering scaffolds.[16,17] The favorable interaction of HCASMCs with these materials will be a necessary condition in enabling the attachment, proliferation, and differentiation of cultured cells. Although a number of classes of PEAs have been previously reported,[18−20] the particular PEAs of interest in this work are composed of α-amino acids, diols, and dicarboxylic acids. As their backbones contain both ester and amide linkages they can undergo both hydrolytic and enzymatic degradation where suitable monomer selection can provide nontoxic metabolic intermediates upon degradation. Another attractive feature of these PEAs is that their biological and mechanical properties can be readily tuned by the crystallinity, hydrophobicity and chemical functionality of their constituent monomers.[21] In the current study, Langmuir−Blodgett (LB) technology was used to prepare ultrathin films of three different PEAs on waveguide substrates and the average number of cell adhesions (focal and close contacts) formed by HCASMCs were determined as a function of the polymer structure and cell culture conditions. The data obtained from WEFF microscopy are compared with quantitative data obtained by immunostaining for vinculin, which is a focal adhesion component localized to adhesive plaques. The attachment, spreading, and morphology of HCASMCs on PEA films were also evaluated.

MATERIALS AND METHODS

Waveguide Evanescent Field Fluorescence (WEFF) Microscopy. The WEFF microscope which is described elsewhere[14] consists of an inverted microscope (Carl Zeiss, Oberkochen, Germany), where the specimen was placed on top of the waveguide. A HeNe laser (λ = 543 nm) was coupled into a waveguide mode by a grating located on the waveguide. In order to block the undesired excitation wavelength, a long pass filter with a cutoff wavelength of λ_{cutoff} = 560 nm was fitted between the objective and the camera. The camera was connected to the computer on which the images were processed with Image-Pro 6 software. Bright-field microscopy images of the sample were captured with the same field of view as the WEFF microscopy images to enable counting of cells.

Waveguide Fabrication. Step-index waveguides were fabricated from SG11 glass slides (Schott, Grünenplan, Germany). The glass slides were first sonicated in a 2% Hellmanex solution (Hellma, Müllheim, Germany) in deionized (DI) water for 15 min and then rinsed followed by a further sonication with DI water. The rinse and sonication steps were repeated with anhydrous ethanol. Following this cleaning procedure, the glass slides were placed in molten $AgNO_3$ (EMD Chemicals, Gibbstown, NJ, U.S.A.) in a tube furnace (Yokogawa Meters and Instruments Corporation, Tokyo, Japan). This enabled ion exchange to occur at the interface of the glass slide and molten salt. After ion exchange, the glass slides were removed from the melt, cooled with nitrogen gas under ambient conditions, thoroughly rinsed and sonicated for 30 min in Milli-Q water.[13] A waveguide mode coupling grating was fabricated by a holographic laser set-up in photoresist.[22] Multimode waveguides with thicknesses of 500−600 nm and gratings with periodicities (Λ) in the order of 530−550 nm and 600−650 nm were achieved

Preparation of Ultrathin Langmuir−Blodgett (LB) Poly(ester amide) (PEA) Films for Cell Culture. The syntheses and characterization of the PEAs are described elsewhere.[17] PEAs **1−3** (Scheme 1) were dissolved in chloroform at a concentration of 1.0 mg/mL. The solutions were sonicated to promote dissolution and then filtered through a 0.2 μm syringe filter. The LB film preparation parameters were identical for all PEAs: LB trough, KSV 3000 (KSV Nima, Espoo, Finland); spread volume, 200 μL; compression rate, 5 mm/min; film lift speed, 2 mm/min; and surface pressure (Π) at deposition, 2 mN/m. The substrates used for film transfer were the waveguides, which were first cleaned with 70% ethanol followed by a rinse with Milli-Q water. The waveguides were mounted in the water phase of the trough before spreading the polymer solution. The polymer solution was then carefully spread onto the Milli-Q water subphase with a Hamilton microliter syringe. After solvent evaporation, the barriers were moved to achieve a surface pressure

of 2 mN/m. The LB transfer took place with the waveguide substrate oriented perpendicular to the barrier direction, to allow for stretching of the aggregates.

LB Film Characterization. LB films prepared from PEAs were viewed under dark-field light microscopy (Axioskope-2 MAT, Carl Zeiss, Oberkochen, Germany) to examine the homogeneity of the films before cell seeding and culturing. Film thicknesses were determined by interference between light reflecting from the surface and light traveling through the film using variable angle spectroscopic ellipsometer (M2000 V, J.A. Woollam, Lincoln, NE). For comparative purposes, film thicknesses were also measured by Dektak 3 surface profilometer and atomic force microscopy (AFM) (both from Veeco Instruments, Santa Barbara, CA).

Cell Culture. Primary HCASMCs were purchased from Lonza Walkersville, Inc. (Walkersville, MD, USA) and used between passages 5 and 9. HCASMCs cultured in serum were grown in smooth muscle cell basal medium (SmBM, Lonza Walkersville, Inc., Walkersville, MD, USA) supplemented with smooth muscle cell growth medium-2 (SmGM-2, SingleQuots; Lonza Walkersville Inc., Walkersville, MD, USA). HCASMCs cultured in the absence of serum were grown in BioWhittaker PC-1™ base medium (Lonza Walkersville, Inc., Walkersville, MD, USA) supplemented with PC-1™ sterile supplement (Lonza Walkersville Inc., Walkersville, MD, USA) and L-glutamine (2 mM, Invitrogen Canada Inc., Burlington, ON, Canada). All cultures were maintained at 37 °C in a humidified incubator containing 5% CO_2. Culture media was replaced at day 1 and every other day thereafter.

Cell Culture for WEFF Microscopic Analysis. Waveguides were sterilized with 70% ethanol for 30 min and were allowed to dry for 30 min under germicidal UV light. HCASMCs were then seeded directly onto the surface of the PEA LB films or control waveguides at a density of 10,000 cells/waveguide and cultured up to 80% confluency (typically for 3 or 4 days). The cells were fixed at ambient temperature for 10 min in 4% formaldehyde (0.5 mL; EMD Chemicals, Gibbstown, NJ, USA) in phosphate-buffered saline (PBS), followed by 2 washes in PBS. The cell membrane labeling solution was prepared by adding 5 μL of the lipophilic dye solution −1,1′-dioctadecyl-3,3,3′,3′-tetramethylindocarbocyanine perchlorate in ethanol (Vybrant DiI cell-labeling solution, Invitrogen Canada Inc., Burlington, ON, Canada) to 1 mL of normal growth medium. The labeling solution (100 μL) was added and gently agitated to cover the cell-seeded waveguides and then incubated at 37 °C for 20 min. The staining medium was then drained off and replaced with fresh media and incubated for a further 10 min. The cells were washed three times with normal growth medium prior to microscopic analysis.

Fluorescence Microscopy. Polymer films were obtained by twice dip-coating 12 mm diameter glass coverslips into 1% (wt) solutions of the PEAs in DMF and were dried at 60 °C under reduced pressure overnight. One glass coverslip was placed in each well of a 24-well culture plate. The films were sterilized with 70% ethanol for 30 min and then exposed to germicidal UV for 1 h, prior to conditioning overnight in Hank's Balanced Salt Solution (HBSS, 0.5 mL; Invitrogen Canada Inc., Burlington, ON, Canada). For examining HCASMC morphology, the HCASMCs were seeded directly on the surface of the dip-coated PEA films at a density of 15 000 cells/cm^2 and cultured in the presence of serum for 24 h prior to fixation and staining as described below. For vinculin immunostaining studies, natural, human fibronectin (FN, 2 μg/cm^2; Santa Cruz Biotechnology Inc., Santa Cruz, CA, USA) in HBSS was adsorbed to glass coverslips for 1 h and the resulting surfaces served as positive controls. All cells were seeded directly on the surface of the PEA or FN coated coverslips at a density of 2000 cells/cm^2 and cultured in the presence or absence of serum for 24 h (serum) or 4 days (serum-free). Cells were washed with prewarmed PBS before fixation with a 4% formaldehyde solution (1 mL; EMD Chemicals, Gibbstown, NJ, USA) in divalent cation-free PBS at ambient temperature for 10 min. Following 3 washes in PBS, HCASMCs were permeabilized with 0.1% Triton X-100 (0.5 mL; VWR International, Mississauga, ON, Canada) in PBS for 5 min and again washed 3 times with PBS. The HCASMCs were incubated with 1% bovine serum albumin (BSA) in PBS (0.5 mL; Sigma-Aldrich, Oakville, ON, Canada) for 30 min at ambient temperature prior to their incubation with monoclonal antivinculin (SPM227, 1:50 dilution; Abcam, Cambridge, MA, USA) for 1 h. Following 3 washes in PBS, the HCASMCs were then incubated in the dark for 1 h at ambient temperature with Alexa Fluor 488-conjugated goat antimouse IgG (1:300 dilution; Invitrogen Canada Inc., Burlington, ON, Canada). Following 3 washes in PBS, the HCASMCs were further incubated in the dark at ambient temperature with Alexa Fluor 568-conjugated phalloidin (1:50 dilution; Invitrogen Canada Inc., Burlington, ON, Canada) for 20 min in a 1% BSA/PBS solution followed by another 3 washes with PBS. The HCASMCs were then counterstained with 4′-6-diamidino-2-phenylindole dyhydrochloride (DAPI, 300 nM in PBS, 0.5 mL; Invitrogen Canada Inc., Burlington, ON, Canada) for 10 min to label the nuclei and again washed 3 times with PBS. The coverslips were mounted on microscope slides with ProLong Gold antifade reagent (Invitrogen Canada Inc., Burlington, ON, Canada), dried overnight at room temperature in the dark, prior to sealing with nail enamel. Samples were analyzed with a Zeiss LSM 5 Duo confocal microscope with 9 laser lines and appropriate filters (Carl Zeiss, Oberkochen, Germany).

Statistical Analyses. The statistical data are given as the mean ± standard error for experiments conducted at least in triplicate. Differences between two groups were compared using a two-tailed unpaired student's *t*-test with GraphPad Prism 4, where values of $p < 0.05$ were considered statistically significant.

RESULTS AND DISCUSSION

Although a diverse array of PEAs have been previously reported by our group[16,17,21,23] and others[20,24−27] and recently reviewed,[28,29] PEAs **1**−**3** depicted in Scheme 1 were selected for this investigation. This was in part due to their solubility in chloroform, a solvent compatible with LB technology; whereas, many previously synthesized PEAs are only soluble in water-miscible solvents such as *N*,*N*-dimethylformamide (DMF).[30] In addition, PEAs **1**−**3** are currently under investigation in our group as viable materials for the development of tissue engineering scaffolds. PEAs **1**−**3** all contain sebacic acid and L-phenylalanine. PEA **1** contains 1,4-butanediol, whereas PEA **2** contains 1,8-octanediol and is therefore slightly more hydrophobic. In PEA **3**, 10 mol % of the L-phenylalanine was randomly substituted with L-lysine. This PEA was of interest because the cationic amines of the lysine moieties could be used to promote cell adhesion[31] or to conjugate biomolecules that regulate cell growth, differentiation and other signaling pathways.[32] The molecular weight data of the specific batches of PEAs used in this study are provided in Table 1.

Table 1. Molecular Weight and Polydispersity Indices of PEAs 1−3

PEA	number average mol wt, M_n (g/mol)	weight average mol wt, M_w (g/mol)	polydispersity index
1	53 500	103 000	1.92
2	65 600	89 100	1.36
3	20 700	44 700	2.15

Given that the evanescent field decays beyond 70 nm, the polymer film thickness needed to be less than 20 nm to observe cell adhesion to the various PEA surfaces. This film thickness could not be achieved by solvent casting. Alternatively, spin-coating was attempted but also proved unsuccessful because the gratings on the waveguides were undesirably covered by the PEA films. The above difficulties were addressed by using LB technology to obtain ultrathin PEA films (Table 2). Polymers are used in LB technology despite their long chains, inherent

Table 2. Film Thicknesses of PEA 1 from Different LB Film Preparation Conditions

LB film preparation conditions			film thickness			
spread volume (μL)	concentration (mg/mL)	surface pressure, Π (mN/m)	ellipsometry (nm)	Dektak (nm)	AFM (nm)	roughness (AFM) (nm)
300	1.0	5	14.4–14.6	16.9–17.9		
300	1.0	10	15.8–16.0	11.0–12.0		
300	0.5	10	13.0–16.0		12.0–14.0	0.28–0.45
200	1.0	10	20.0–21.0		13.0–15.0	0.40–0.45

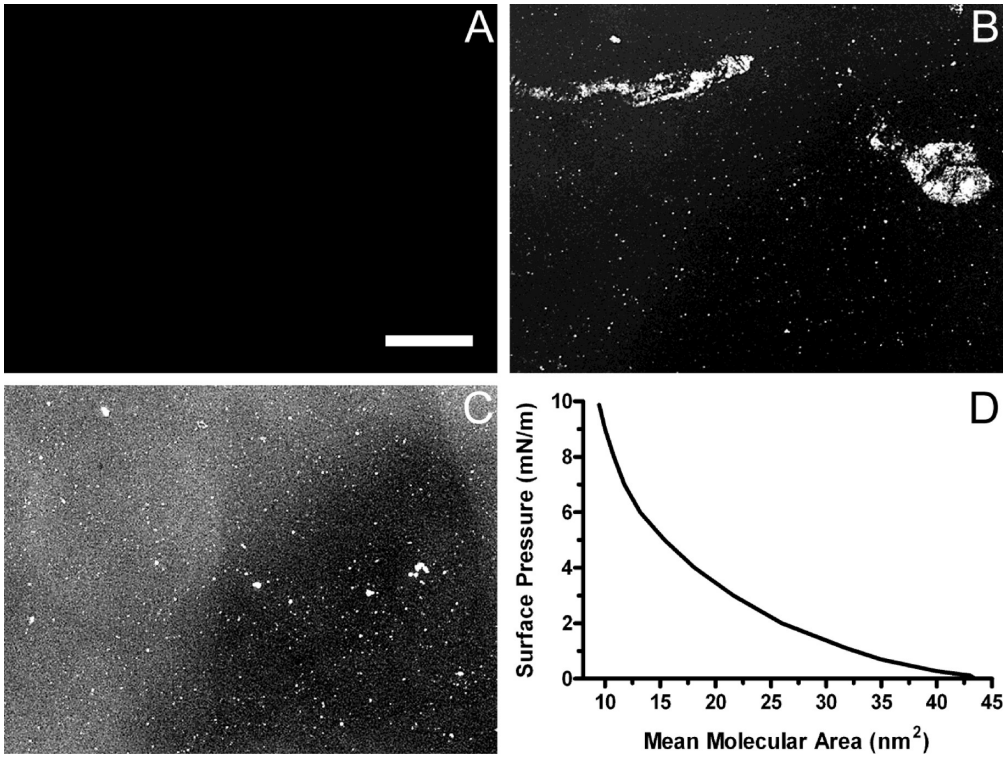

Figure 1. Dark-field microscopy images of (A) a bare waveguide, (B) LB film of PEA **1** obtained using DMF, (C) LB film of PEA **1** obtained using chloroform. (D) Surface pressure isotherm for PEA **1** from a solution in chloroform. Scale bar applicable to A, B, and C represents 200 μm.

polydispersity, high viscosity, and strong intra- and intermolecular interactions. For example, intra- and intermolecular hydrogen bonding of the amide groups of these PEAs could potentially lead to aggregate formation.[33] As aggregates deposited onto the waveguide at low pressure can result in the formation of a nonclosed and nonuniform film, each PEA solution was transferred to the waveguide perpendicular to the barrier direction. This technique facilitated stretching of the aggregates minimizing inhomogeneities in the PEA film transfer, which otherwise could result in uncoated areas on the waveguide. Despite this approach to minimize inhomogeneities in preparing LB films of the PEAs, those prepared from DMF resulted in aggregation and inhomogeneous distribution over the substrate as evidenced by the clustering of bright spots in Figure 1B. This is attributed to DMF's slow evaporation and miscibility with the subphase. However, PEA LB films obtained from a chloroform solution were more evenly distributed on the subphase and the films formed more homogeneously as the scattering spot distribution shows (Figure 1C). Unlike typical LB monolayers, when the PEAs were compressed by the barriers they did not collapse, even when the barriers were near complete closure. This is evident in the isotherm as depicted for PEA **1** in Figure 1D, which has no steep decline or peak corresponding to a collapse of the solid phase at small mean molecular areas. Similar isotherms with even lower mean molecular areas were obtained with PEA **2** and PEA **3** (see the Supporting Information, Figure 1A, B). Further compression led to an undesirable thick smear between the barriers of the LB trough resulting from stacked PEA chains. Consistent with the present study, such stacked and noncollapsing films at increased compression (corresponding to small mean molecular areas) were also reported for collagen.[34]

Not surprisingly, these PEA LB films did not perform like classic LB films. Aggregates were visible on the subphase which may have been the result of strong intra- and intermolecular interactions (Figure 1B, C). These aggregates were floating into and upon each other, and the increase in the surface pressure during compression of the barriers was caused by an increase in packing density of the aggregates. An increase in the thickness of the film must be accompanied by this pressure increase. Therefore, when preparing LB films with these PEAs, the layer formed on the subphase is not a monolayer, but most likely a multilayer (Table 2).

Previously nonclassic LB behavior with aggregate formation was observed for collagen due to strong intermolecular interactions.[34] Because the spacer diol chain between the adjacent amide bonds is short for PEA **1** (Scheme 1) compared with PEA **2** and PEA **3**, the formation of a multilayer rather than a monolayer is likely for PEA **1**. This increased density of amide bonds due to the short chain diol chain could yield more

hydrogen bonding and an increase in film viscosity. In contrast, PEAs **2** and **3** have a longer diol chain and therefore have fewer possibilities for intra- and intermolecular hydrogen bonding resulting in less viscous films. In addition to this longer diol chain, PEA **3** has an L-lysine side chain that allows free rotation, resulting in weaker intermolecular bonding. As presented in Table 2, film thicknesses of LB films of PEA **1** were less than 20 nm when the spread volume was maintained at 300 μL. A surface pressure change from 5 to 10 mN/m and a PEA concentration change from 0.5 mg/mL to 1 mg/mL did not have any appreciable effect on the film thicknesses. Although film thickness data varied between ellipsometry and AFM measurements for a spread volume of 200 μL, it appeared that a higher film thickness resulted from a lower spread volume, at least on the basis of the ellipsometry data.

To examine and quantify HCASMC adhesion to these PEAs, two approaches were adopted − WEFF microscopy to observe cell adhesion to the substratum and vinculin immunostaining to illustrate possible integrin-mediated HCASMC focal adhesion. For WEFF microscopy analyses, cells were grown on LB films until 80% confluent (typically 3−4 days). The LB technology for film formation was necessary because the total thickness of the PEA film and the cell membrane should not exceed the penetration depth of the evanescent field of the manufactured waveguides, which decays within roughly 70 nm. By staining the cell membranes with the fluorescent dye, DiI, the areas of the cells that are closest to the surface of the waveguide, are the most strongly excited and fluorescent, while those areas outside the evanescent field do not fluoresce. In illuminating only this interfacial area, the number of attachment sites per HCASMC could then be determined by counting the bright spots appearing in the WEFF microscopy images using ImageJ software (National Institutes of Health, Bethesda, MD, USA) and dividing it by the number of cells present. Figure 2 shows representative images of HCASMCs cultured on the control waveguide and PEA LB films taken with bright field and WEFF microscopy. In the bright field images (left), individual cells are well-spread. The white spots in the corresponding WEFF images (right) show the sites of cell attachment to the PEA LB films. The number of cells on the control waveguide (Figure 2A and B) appeared to be lower than those on the PEA LB films suggesting that the PEAs provided a better environment for HCASMC attachment and spreading. The WEFF image of the control waveguide (Figure 2B) does not exhibit any epi-fluorescence because of the absence of the PEA film. The PEA films located in the area of the highest evanescent fields of the waveguide are the primary source of scattered excitation photons (compare with Figure 1C). These scattered photons can reach all areas of the cell, including those outside the evanescent field and excite fluorescence photons. While the WEFF images of the PEA-coated waveguides illustrate predominantly the evanescent information and hence the contact points of the cell, (Figure 2D, F, H), it could also show a nebulous background outlining the cell body due to this epi-fluorescence. Epi-fluorescence which is also a common observation in TIRF can be removed from WEFF images by choosing smaller integration times, but the cell outline information will be lacking.[13]

An analysis of the number of adhesions that the HCASMCs formed on both the control waveguide and PEA LB films was first conducted in the presence of serum in the culture media. As shown in Figure 3, few cell adhesion sites on the control waveguide were observed. Although the waveguide was not

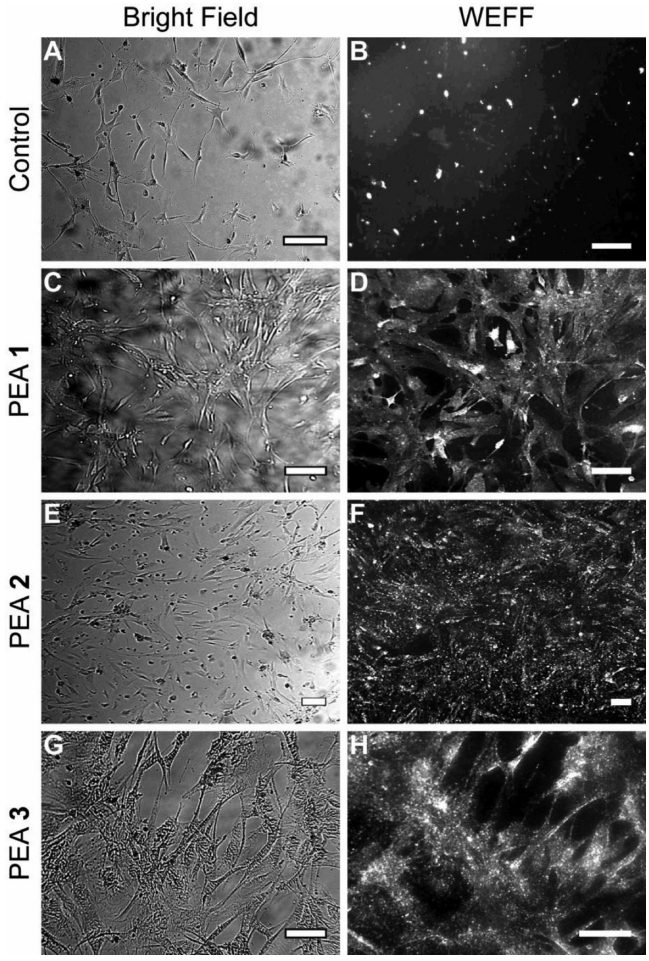

Figure 2. Bright-field and corresponding WEFF microscopy images of (A, B) HCASMCs seeded on the control waveguide and (C, D) LB films of PEA **1**, (E, F) PEA **2**, and (G, H) PEA **3**. HCASMCs were cultured until 80% confluent, fixed and stained using DiI prior to imaging. Scale bars represent 200 μm.

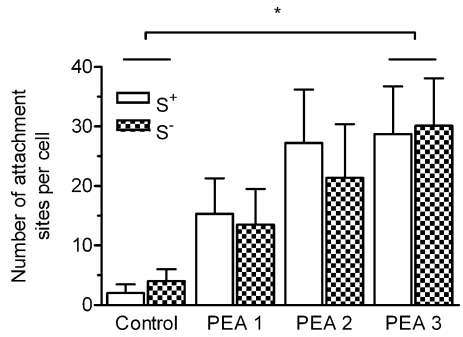

Figure 3. Average number of attachment sites per cell on control waveguides and on PEA LB films cultured in serum-containing (S^+) or serum-free (S^-) media. * denotes statistical significance ($p < 0.05$).

expected to be an ideal substrate for cell culture, the adsorption of proteins on a surface is often considered the first step toward the adhesion of cells on that surface.[3] In particular, the serum used in cell culture contains many cell adhesive proteins including fibronectin and vitronectin, which may promote the formation of differential focal adhesions.[31] Therefore, the role of protein adsorption in the establishment of adhesions of HCASMCs on the waveguides was also evaluated by culturing

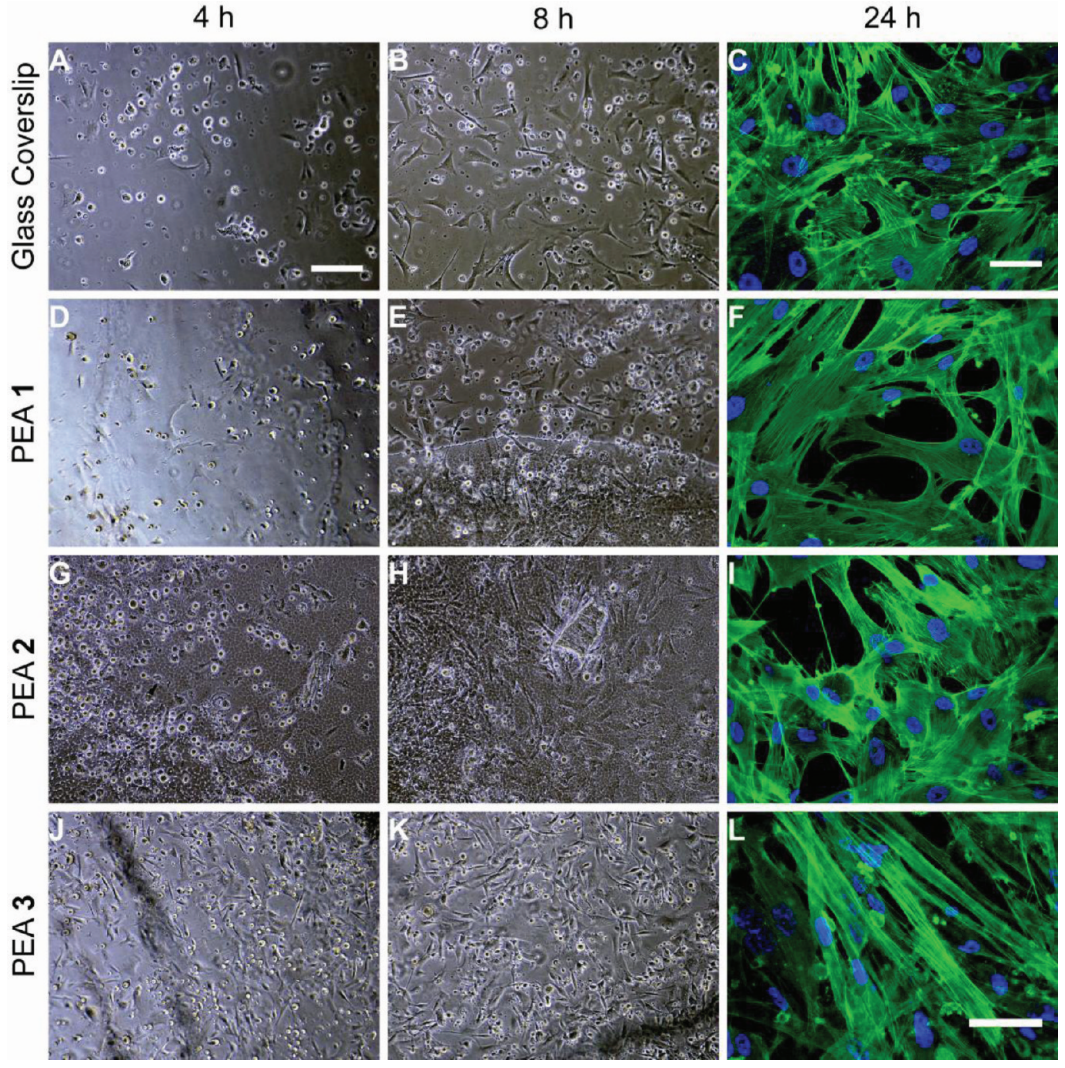

Figure 4. Phase contrast and confocal microscopy images of HCASMCs cultured on PEA films. Cells were seeded at 15 000 cells/cm^2 and cultured for up to 24 h in serum-containing (S^+) media. Phase contrast images were taken at 4 and 8 h; whereas, the confocal microscopy images were taken after 24 h of culture. HCASMC F-actin (green) and nuclei (blue) are shown in the confocal images (C, F, I, L). Phase contrast scale bar represents 200 μm, whereas confocal microscopy image scale bars represent 50 μm. Glass coverslips served as controls.

cells in the absence of serum. On the control waveguides, this resulted in an average of 0.9 attachment sites per cell. This result was not statistically significant ($p > 0.05$) from the serum-containing (S^+) media study of 2.1 attachment sites per cell indicating protein adsorption did not play a significant role in HCASMC adhesion to the control waveguides. Moreover, the number of attachment sites in both S^+ and S^- control waveguides appeared to be lower than those obtained from immunostaining studies reported in the literature (at least 5−10 focal adhesions per cell) for various cell types on different materials.[35−38] In generating a waveguide on the surface of a glass slide, low polarizability ions (sodium) are exchanged for high polarizability ions (silver) to enhance the refractive index on the surface. Given that the waveguide surfaces are silver ion-exchanged, reduced attachment sites are attributed to residual silver ions which are known to reduce cell adhesion.[39] However, the presence of the LB PEA films may have masked the detrimental effects of the residual silver ions on cell adhesion. In addition to focal adhesions, there is a potential for cells to also form nonfocal contacts such as close contacts.[38] Although close contacts typically range from 20 to 50 nm from the substratum, the ventral cell membrane of the HCASMCs may remain equidistant from the surface, as previously reported with retinal pigment epithelial cells,[40] inhibiting effective isolation and segregation of individual close contacts, arbitrarily underestimating the number of cell attachment sites. We did not distinguish between focal contacts and close contacts as the distances of the individual contacts were not investigated in this study.

Not only did the presence of serum not influence the number of attachment sites in the control waveguide, this behavior was also seen in all three PEA LB films as no statistical significance was observed among them ($p > 0.05$, Figure 3). In the S^+ culture, PEA **1** exhibited 15.3 ± 6 adhesions per cell, which was high but not significantly different from the control waveguide. PEA **2** exhibited 27.2 ± 9 adhesions per cell suggesting that the increased hydrophobicity imparted by the longer chain diol created a more favorable environment for cell attachment, potentially due to increased protein adsorption. However, due to the relatively high standard error associated with the measurements, these results were not statistically different. PEA **3** containing the lysine moiety exhibited a similar

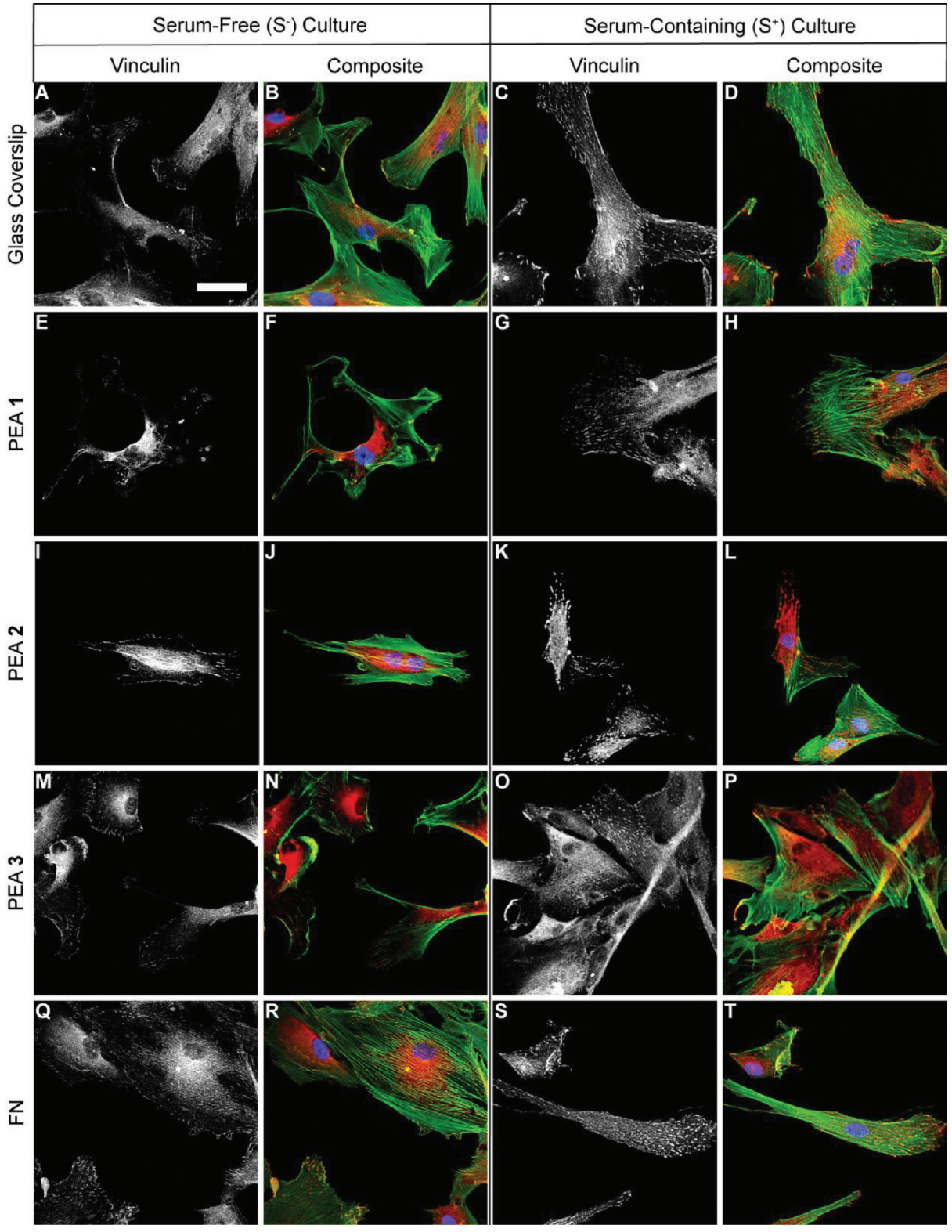

Figure 5. Confocal microscopy images of (A–D) vinculin immunostained HCASMCs on glass coverslips, (E–P) PEA films, and (Q–T) FN-coated coverslips in the absence or presence of serum. Black and white images show vinculin immunostaining only, while fluorescence labeling of HCASMC F-actin (green), vinculin (red), and nuclei (blue) are all shown in the composite images. Scale bar represents 50 μm.

number (28.7 ± 8) of cell adhesions to PEA **2**, the same polymer lacking the incorporation of the lysine residues. While the presence of cationic lysine residues was expected to result in increased cell adhesion based on previous reports,[31,41] the WEFF microscopy results suggest that the number of lysine moieties incorporated into these polymers may not have been sufficient to significantly increase the number of cell adhesion sites. However, the number of adhesion sites of the HCASMCs on PEA **3** in both S^- and S^+ culture was significantly higher than the control waveguides ($p < 0.05$). This result may

dx.doi.org/10.1021/am201582q | *ACS Appl. Mater. Interfaces* 2012, 4, 1303–1312

indicate the cationic nature of the lysine residues of PEA **3** is engaged in nonspecific electrostatic binding with the negatively charged glycocalyx layer on the cell surface in the absence of serum. In S^+ culture, the cationic amine groups of PEA **3** may also bind electrostatically with cell adhesive proteins such as fibronectin or vitronectin, which carry net negative charges at physiologic conditions as their isoelectric points are 5.6−6.1 and 4.8−5.0 respectively, thereby also enhancing cell adhesion.[31,42] Ultimately, the number of attachment sites observed in the comparative serum study, suggests that for all substrata, protein adsorption did not play a major role in the establishment of cell adhesions.

After evaluating the potential use of WEFF microscopy for determining the number of cell attachment sites on PEA LB films, we compared the data with vinculin immunostaining, which is a well-established method for quantifying focal adhesions. To achieve this, we cultured HCASMCs on solvent-cast PEAs films. Initially, a time-course analysis was conducted using phase contrast microscopy to ensure HCASMC attachment and spreading on the solvent cast PEA films, prior to their immunostaining (Figure 4). To emulate the expected cell density on the waveguides after 3 or 4 days culture, we seeded cells at 15 000 cells/cm^2 on the solvent cast PEA films. Four hours after seeding, most cells adhered to the surface (including the glass coverslip control), but remained spherical in shape with little evidence of spreading (Figure 4A, D, G, J). However, after 8 h, cell spreading was observed on all materials as judged by the flat morphology and larger contact areas occupied by individual cells (Figure 4B, E, H, K). Given that the surfaces were not coated with cell adhesive proteins, the observed spreading is likely attributed to the surface adsorption of serum proteins from the culture media. To confirm this, we cultured cells in the absence of serum and evaluated cell spreading. The data (see the Supporting Information, Figures 2 and 3) suggest that cell attachment and spreading on the PEAs is retarded when compared with those cultured in the presence of serum as cell spreading only became evident at 24 h of culture, presumably due to cell-secreted adhesive proteins. Although this was not entirely unexpected, it suggests that these PEAs can support attachment of HCASMCs even in the absence of serum. Complete HCASMC spreading and their cell−cell contact formation is seen following 24 h of S^+ culture as presented by the confocal microscopy images (Figure 4C, F, I, L). It is noted that favorable cell-substratum adhesion is required for subsequent cellular responses such as proliferation and differentiation.

Given that HCASMCs were well-spread on all PEA films after 24 h, we then examined whether these cells could form focal contacts also known as focal adhesions (FAs), which are specialized sites of adhesion between the cell and the substrate. In addition to anchoring cells, focal adhesion proteins are involved in integrin signaling that activates various intracellular signaling pathways that direct cell viability, proliferation, and differentiation. Although there are many proteins involved in FAs, vinculin is the most studied and well-understood actin-binding protein;[4,43] therefore, we immunostained for vinculin and quantified the number of HCASMC focal contacts. As shown in Figure 5, HCASMCs expressed vinculin in both S^- and S^+ culture media. However, the vinculin appeared to be concentrated at the cell periphery for the S^- cultures with the exception of the fibronectin coated control cultures (Figure 5A, E, I, M). The rationale for using fibronectin was due to its cell adhesive RGD peptide motif, which served as a positive control. In the presence of serum, the vinculin was distributed uniformly throughout the cell body (Figure 5C, G, K, O). For the fibronectin treated positive control cultures, the distribution of vinculin seems to be independent of serum (Figure 5Q, S). Because vinculin is localized on the cytoplasmic face of integrin-mediated cell−extracellular matrix junctions,[43] HCASMCs cultured on these fibronectin coated controls appear to be making more focal contact areas than on the PEA surfaces.

In order to gain further insight into these cultures, the number of FAs per cell and per unit area of cell on the PEA films were determined (Figure 6A, B), where the number of

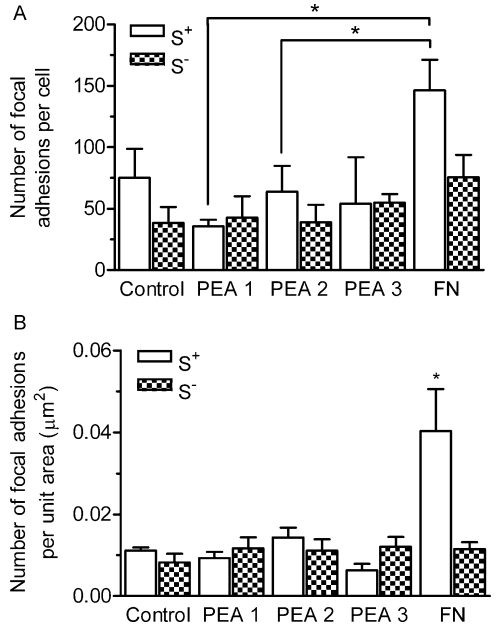

Figure 6. Number of focal adhesions (A) per HCASMC and (B) per unit area (μm^2) on the PEA films in serum-containing (S^+) and serum-free (S^-) media. The * denotes statistical significance ($p < 0.05$).

focal contacts and cell area were both calculated using ImageJ software. In the S^+ cultures, there was a significant increase in FAs in the fibronectin coated control cultures compared with both PEA **1** and PEA **2**, but not PEA **3** likely due to the scatter in data that introduced a relatively large error in this case. This scatter in the data is in part attributed to those cells fixed in the process of migration as they tend to form extensive close contacts,[44] which under-express vinculin.[40] This data, however, is consistent with the immunostaining findings, where HCASMCs formed more FAs with the fibronectin coated controls (Figure 5S, T). Although the fibronectin coated control in the S^+ culture exhibited an increased number of focal adhesions, there was no statistical significance in the number of FAs per cell on all other materials tested regardless of culture conditions ($p > 0.05$). Similarly, the number of focal adhesions per unit area on all the materials cultured in serum is significantly lower than the fibronectin coated controls ($p < 0.05$). However, fibronectin had no significant effect on the number of focal adhesions per unit area in the absence of serum ($p > 0.05$). In comparison to the WEFF data presented in Figure 3 where PEA **3** showed a statistically significant increase in the number of attachment sites per cell, the immunostaining data (Figure 6) did not show significance between the control and PEA **3**. This difference is attributed to the two different control surfaces used in the respective experiments. For reasons

mentioned earlier, the WEFF control experiments were done on silver ion-exchanged glass slides needed to form a waveguide, whereas the immunostaining experiments were conducted using conventional cell culture glass coverslips.

Overall, an average of 35−64 FAs per HCASMC cultured on PEA films calculated from vinculin immunostaining are consistent with the WEFF microscopy data. Although the WEFF microscopy data shown in Figure 3 (average attachment sites of 15−29 per cell) are slightly lower than the vinculin immunostaining data shown in Figure 6 (average focal adhesions of 35−64 per cell), there is no statistical significance among any of the PEAs tested in either serum-containing or serum-free culture media ($p > 0.05$). In addition, these results compare favorably with literature data.[45−48] For example, for fibroblasts, an average of 20−30 FAs per cell is reported;[35,36] whereas, for myoblasts an average of 70 FAs per cell is reported.[37,49] It also appears that FAs per cell is dependent on the culture substrates used where stiff surfaces had higher FAs per cell than flexible substrates. For example, fibroblasts cultured on graphene and carbon nanotubes had more than 100 FAs per cell;[50] whereas, the same cells cultured on a standard culture dish had 20 FAs per cell, whereas lung fibroblasts seeded on silicone rubber had 5 FAs per cell.[45] Finally, a decrease in the FAs per cell from 20−5 is reported for HT-1080 cells cultured in 3D surfaces.[47] In view of these reported values, our data on solvent cast PEA films are within the expected range. Furthermore, given that HCASMCs were making focal adhesions on these PEAs, it suggests these materials can promote integrin signaling, which is critical to cell migration and differentiation.

CONCLUSIONS

In this study, we investigated the adhesion of HCASMCs to PEA films using WEFF microscopy and compared it with a conventional vinculin immunostaining technique. The WEFF microscopy work required the preparation of ultrathin films of the PEAs on waveguide surfaces by LB technology, an aspect that was challenging due to the hydrogen bonding capabilities of the PEAs resulting in their propensity to aggregate. Despite this challenge, 20 nm thick PEA films were successfully prepared. The WEFF results indicated that all PEAs deposited on the waveguides enhanced HCASMC adhesion compared with the uncoated control waveguides. However, due to the relatively high standard error in the WEFF data, only the cationic PEA was significantly higher than the control waveguide. The quantification of vinculin immunostaining supported the WEFF microscopy data, as there was no statistical difference in the number of focal adhesions per cell or per unit area among the PEAs tested regardless of culture conditions. Only the fibronectin coated controls in serum-containing media exhibited a significantly higher number of focal adhesions per cell and per unit area. The presence of these focal adhesions implies that all these PEAs promote integrin-mediated signaling, a crucial step in cell migration and proliferation. Taken together, our results demonstrate the promise of PEA surfaces for the attachment of HCASMCs and suggest that a diverse range of PEAs can potentially be used for vascular tissue engineering applications.

ASSOCIATED CONTENT

Supporting Information

Surface pressure isotherms of PEAs **2** and **3** from solutions in chloroform; time series human coronary artery smooth muscle cell (HCASMC) attachment up to 24 h on dip-coated poly(ester amide) (PEA) films in serum-containing (S^+) and serum-free (S^-) culture. This material is available free of charge via the Internet at http://pubs.acs.org.

AUTHOR INFORMATION

Corresponding Author

*E-mail: kmequani@uwo.ca. Tel: +1 (519) 661-2111, ext. 88573. Fax: +1 (519) 661-3498.

ACKNOWLEDGMENTS

The authors acknowledge the financial support provided by the Heart and Stroke Foundation of Canada (HSFC) and Natural Sciences and Engineering Research Council (NSERC) of Canada. C.H. and D.I. acknowledge the RheinMain University for travel grants.

REFERENCES

(1) Niu, X. F.; Wang, Y. L.; Luo, Y. F.; Xin, J.; Li, Y. G. *J. Mater. Sci. Technol.* **2005**, *21*, 571−576.
(2) Storrie, H.; Guler, M. O.; Abu-Amara, S. N.; Volberg, T.; Rao, M.; Geiger, B.; Stupp, S. I. *Biomaterials* **2007**, *28*, 4608−4618.
(3) Bačáková, L.; Filová, E.; Rypáček, F.; Švorčík, V.; Starý, V. *Physiol. Res.* **2004**, *53*, S35−S45.
(4) Lo, S. H. *Dev. Biol.* **2006**, *294*, 280−291.
(5) Burmeister, J. S.; Olivier, L. A.; Reichert, W. M.; Truskey, G. A. *Biomaterials* **1998**, *19*, 307−325.
(6) Burmeister, J. S.; Truskey, G. A.; Reichert, W. M. *J. Microsc.* **1994**, *173*, 39−51.
(7) Giebel, K. F.; Bechinger, C.; Herminghaus, S.; Riedel, M.; Leiderer, P.; Weiland, U.; Bastmeyer, M. *Biophy. J* **1999**, *76*, 509−516.
(8) Verschueren, H. *J. Cell Sci.* **1985**, *75*, 279−301.
(9) Braun, D.; Fromherz, P. *Appl. Phys. Mater. Sci. Process.* **1997**, *65*, 341−348.
(10) Agnarsson, B.; Ingthorsson, S.; Gudjonsson, T.; Leosson, K. *Opt. Express* **2009**, *17*, 5075−5082.
(11) Grandin, H. M.; Städler, B.; Textor, M.; Vörös, J. *Biosens. Bioelectron.* **2006**, *21*, 1476−1482.
(12) Hassanzadeh, A.; Armstrong, S.; Dixon, S. J.; Mittler, S. *Appl. Phys. Lett.* **2009**, *94*, 033503.
(13) Hassanzadeh, A.; Nitsche, M.; Armstrong, S.; Nabavi, N.; Harrison, R.; Dixon, S. J.; Langbein, U.; Mittler, S. *J. Biomed. Opt.* **2010**, *15*, 036018.
(14) Hassanzadeh, A.; Nitsche, M.; Mittler, S.; Armstrong, S.; Dixon, J.; Langbein, U. *Appl. Phys. Lett.* **2008**, *92*, 233503.
(15) Horvath, R.; Pedersen, H. C.; Skivesen, N.; Selmeczi, D.; Larsen, N. B. *Appl. Phys. Lett.* **2005**, *86*, 071101.
(16) Karimi, P.; Rizkalla, A. S.; Mequanint, K. *Materials* **2010**, *3*, 2346−2368.
(17) Knight, D. K.; Gillies, E. R.; Mequanint, K. *Biomacromolecules* **2011**, *12*, 2475−2487.
(18) Bettinger, C. J.; Bruggeman, J. P.; Borenstein, J. T.; Langer, R. S. *Biomaterials* **2008**, *29*, 2315−2325.
(19) Vera, M.; Almontassir, A.; Rodríguez-Galán, A.; Puiggalí, J. *Macromolecules* **2003**, *36*, 9784−9796.
(20) Cheng, H.; Hill, P. S.; Siegwart, D. J.; Vacanti, N.; Lytton-Jean, A. K. R.; Cho, S. W.; Ye, A.; Langer, R.; Anderson, D. G. *Adv. Mater.* **2011**, *23*, H95−H100.
(21) De Wit, M. A.; Wang, Z. X.; Atkins, K. M.; Mequanint, K.; Gillies, E. R. *J. Polym. Sci.: Polym. Chem.* **2008**, *46*, 6376−6392.
(22) Xu, M.; Moshrefzadeh, R.; Gibson, U. J.; Stegeman, G. I.; Seaton, C. T. *Appl. Opt.* **1985**, *24*, 3155−3161.
(23) Atkins, K. M.; Lopez, D.; Knight, D. K.; Mequanint, K.; Gillies, E. R. *J. Polym. Sci.: Polym. Chem.* **2009**, *47*, 3757−3772.
(24) Deng, M.; Wu, J.; Reinhart-King, C. A.; Chu, C. C. *Acta Biomater.* **2011**, *7*, 1504−1515.

(25) Horwitz, J. A.; Shum, K. M.; Bodle, J. C.; Deng, M. X.; Chu, C. C.; Reinhart-King, C. A. *J. Biomed. Mater. Res.* **2010**, *95A*, 371−380.
(26) Pang, X.; Chu, C. C. *Biomaterials* **2010**, *31*, 3745−3754.
(27) Deng, M.; Wu, J.; Reinhart-King, C. A.; Chu, C. C. *Biomacromolecules* **2009**, *10*, 3037−3047.
(28) Sun, H.; Meng, F.; Dias, A. A.; Hendriks, M.; Feijen, J.; Zhong, Z. *Biomacromolecules* **2011**, *12*, 1937−1955.
(29) Rodríguez-Galán, A.; Franco, L.; Puiggalí, J. *Polymers* **2011**, *3*, 65−99.
(30) Fan, Y. J.; Kobayashi, M.; Kise, H. *J. Polym. Sci.: Polym. Chem.* **2001**, *39*, 1318−1328.
(31) Tanahashi, K.; Mikos, A. G. *J. Biomed. Mater. Res. A* **2003**, *67*, 448−457.
(32) DeFife, K. M.; Grako, K.; Cruz-Aranda, G.; Price, S.; Chantung, R.; Macpherson, K.; Khoshabeh, R.; Gopalan, S.; Turnell, W. G. *J. Biomater. Sci., Polym. Ed.* **2009**, *20*, 1495−1511.
(33) Ren, Y.; Zhao, B.; Chai, X.; Lu, A.; Chen, S.; Cao, Y.; Yang, W.; Lu, R.; Duo, J.; Jiang, Y.; Li, T. *Thin Solid Films* **1997**, *293*, 170−174.
(34) Tenboll, A.; Darvish, B.; Hou, W. M.; Duwez, A. S.; Dixon, S. J.; Goldberg, H. A.; Grohe, B.; Mittler, S. *Langmuir* **2010**, *26*, 12165−12172.
(35) Lanning, N. J.; Su, H. W.; Argetsinger, L. S.; Carter-Su, C. *J. Cell Sci.* **2011**, *124*, 3095−3105.
(36) Silberberg, Y. R.; Yakubov, G. E.; Horton, M. A.; Pelling, A. E. *Nanotechnology* **2009**, *20*, 285103.
(37) Yancy, S. L.; Shelden, E. A.; Gilmont, R. R.; Welsh, M. J. *Toxicol. Sci.* **2005**, *84*, 278−286.
(38) Tawil, N.; Wilson, P.; Carbonetto, S. *J. Cell Biol.* **1993**, *120*, 261−271.
(39) Zimmerman, R.; Gurhan, I.; Ozdal-Kurt, F.; Sen, B. H.; Rodrigues, M.; Ila, D. *AIP Conf. Proc.* **2006**, *866*, 329−331.
(40) Fadel, M. P.; Dziak, E.; Lo, C. M.; Ferrier, J.; Mesaeli, N.; Michalak, M.; Opas, M. *J. Biol. Chem.* **1999**, *274*, 15085−15094.
(41) Mazia, D.; Schatten, G.; Sale, W. *J. Cell Biol.* **1975**, *66*, 198−200.
(42) Wolf, H.; Gingell, D. *J. Cell Sci.* **1983**, *63*, 101−112.
(43) Ziegler, W. H.; Liddington, R. C.; Critchley, D. R. *Trends Cell Biol.* **2006**, *16*, 453−460.
(44) Rinnerthaler, G.; Geiger, B.; Small, J. V. *J. Cell Biol.* **1988**, *106*, 747−760.
(45) Boccafoschi, F.; Bosetti, M.; Sandra, P. M.; Leigheb, M.; Cannas, M. *Cell Adhes. Migr.* **2010**, *4*, 19−25.
(46) Ferrari, A.; Faraci, P.; Cecchini, M.; Beltram, F. *Biomaterials* **2010**, *31*, 2565−2573.
(47) Fraley, S. I.; Feng, Y. F.; Wirtz, D.; Longmore, G. D. *Nat. Cell Biol.* **2011**, *13*, 5−7.
(48) Northey, J. J.; Chmielecki, J.; Ngan, E.; Russo, C.; Annis, M. G.; Muller, W. J.; Siegel, P. M. *Mol. Cell. Biol.* **2008**, *28*, 3162−3176.
(49) Thompson, O.; Moore, C. J.; Hussain, S. A.; Kleino, I.; Peckham, M.; Hohenester, E.; Ayscough, K. R.; Saksela, K.; Winder, S. J. *J. Cell Sci.* **2010**, *123*, 118−127.
(50) Ryoo, S. R.; Kim, Y. K.; Kim, M. H.; Min, D. H. *ACS Nano* **2010**, *4*, 6587−6598.